1 **Microinjection, gene knockdown, and CRISPR-mediated gene knock-in in the hard coral,**
2 ***Astrangia poculata***
3
4 Jacob F. Warner[1*], Ryan Besemer [1], Alicia Schickle [2], Erin Borbee[3], Isabella V. Changsut[3], Koty
5 Sharp[2], Leslie S. Babonis[4*]
6
7 **Affiliations:**
8   1. Department of Biology and Marine Biology, UNC Wilmington, Wilmington, NC, 28409
9   2. Feinstein School of Social and Natural Sciences, Roger Williams University, Bristol, RI
10   02871
11   3. Department of Biology, Texas State University, San Marcos, TX, 78666
12   4. Department of Ecology and Evolutionary Biology, Cornell University, Ithaca, NY, 14853
13
14
15 *Correspondence to: Leslie S. Babonis (lsb257@cornell.edu)
16

Summary Statement

21 This study reports the development of the first transgenic knock-in coral, providing the
22 opportunity to track the behavior of various cell types during early coral development.
23
24

Abstract

Cnidarians have become valuable models for understanding many aspects of developmental biology including the evolution of body plan diversity, novel cell type specification, and regeneration. Most of our understanding of gene function during early development in cnidarians comes from a small number of experimental systems including the sea anemone, *Nematostella vectensis.* Few molecular tools have been developed for use in hard corals, limiting our understanding of this diverse and ecologically important clade. Here, we report the development of a suite of tools for manipulating and analyzing gene expression during early development in the northern star coral, *Astrangia poculata.* We present methods for gene knockdown using short hairpin RNAs, gene overexpression using exogenous mRNAs, and endogenous gene tagging using CRISPR-mediated gene knock-in. Combined with our ability to control spawning in the laboratory, these tools make *A. poculata* a tractable experimental system for investigative studies of coral development. Further application of these tools will enable functional analyses of embryonic patterning and morphogenesis across Anthozoa and open new frontiers in coral biology research.

Introduction

Recent advances in the techniques available for genetic manipulation have enabled the ability to perturb and analyze gene function in a broad range of animal phyla (Crawford et al., 2020; Oulhen et al., 2022; Presnell and Browne, 2021; Tinoco et al., 2023). These advancements make it possible to interrogate the evolution of development in taxa representing extreme variation in animal body plans. Among cnidarians, representatives of both Anthozoa (corals, sea anemones, etc) and Medusozoa (hydroids, jellyfish, etc) have emerged as highly tractable experimental systems; however, our understanding of development in these clades arises from investigation of only few species. As an example, the molecular regulation of embryogenesis appears to be well-studied in Anthozoa, yet most of our conclusions about this large and diverse clade of cnidarians derive from studies of the starlet sea anemone, *Nematostella vectensis* (Layden et al., 2016). Investigative studies of gene function in other anthozoans have been challenged by lack of accessibility to gametes, protected status of the adult, and a dearth of molecular tools.

The northern star coral, *Astrangia poculata,* is an attractive experimental organism for research on hard coral (scleractinian) development. This facultatively symbiotic, gonochoristic coral is found in high abundance in coastal waterways from the southern Caribbean to Cape Cod MA, USA (Dimond et al., 2013) and is listed by the IUCN as a species of "least concern". In the late summer, when gametogenesis is at its peak in *A. poculata,* colonies can be collected from near-shore locations, induced to spawn *ex situ,* and their hardy, transparent larvae can be conveniently reared in laboratory conditions (Szmant-Froelich et al., 1980). The considerable ease of access to coral colonies combined with the ability to precisely control the timing of fertilization in the laboratory provides the opportunity to genetically manipulate early-stage embryos. Here, we describe the development of molecular tools for investigating gene function during early development in *A. poculata*. These tools establish *A. poculata* as a tractable research organism for functional studies in corals and, more broadly, as a viable system for comparative studies of cnidarian evolution and development

Results and Discussion

Spawning and microinjection of *Astrangia poculata*

To establish methods for manipulating gene function during embryogenesis in *A. poculata,* we collected wild adult colonies and induced spawning at precise times by raising the water temperature quickly from 19.5°C to 27-28°C in benchtop containers. Gamete release began 1-

76   1.5 hours after heating (**Fig 1A,B**). To perform microinjection, we concentrated fertilized zygotes
77   in a small volume of seawater and pipetted them gently onto the top of a piece of 100μm nylon
78   mesh secured with modeling clay to the bottom of a 35 mm petri dish filled with filtered sea
79   water (**Fig 1C,D**). The nylon mesh serves to cradle the individual zygotes during microinjection
80   and the clay ensures the mesh can be removed easily to facilitate recovery of injected zygotes.
81   At room temperature (~22°C), first cleavage occurs after approximately 90 minutes, allowing for
82   injection of a large number of zygotes. First cleavage in *A. poculata* is holoblastic, resulting in
83   complete segregation of the first two embryonic cells. We demonstrated this by injecting two
84   different dyes at the 2-cell stage and observing conserved segregation of the dyes later in
85   development (**Fig 1E**). By contrast, in *N. vectensis* complete segregation of embryonic cells is
86   not observed until the 8-cell stage (Fritzenwanker et al., 2007). Thus, single-cell injections at the
87   2-cell stage in *A. poculata* could be used to knockdown or overexpress gene products in half of
88   the embryo, facilitating studies of cell-cell communication during early development. To test the
89   feasibility of using exogenous mRNAs for over- and mis-expression assays in *A. poculata*, we
90   injected mRNA encoding a transcription factor (T-cell factor/TCF) isolated from *N. vectensis*,
91   fused to a fluorescent protein (NvTCF-venus) (Röttinger et al., 2012). Blastula stage embryos
92   exhibited nuclear localization of the fluorescent fusion protein as anticipated, and expression
93   was maintained in healthy, dividing cells throughout early development (**Fig 1F**). These results
94   demonstrate robust expression of exogenous transgenes, opening the possibility of using mis-
95   expression approaches to study gene regulatory network diversification across species.
96
97   **Short hairpin RNAs enable efficient gene knockdown**
98   RNA interference techniques have become indispensable for studies of early development as
99   they allow for efficient, robust knockdown of gene function across cell and tissue types. Among
100   cnidarians, RNAi technologies have been successful for manipulating gene function in a wide
101   array of taxa, including both hydrozoans (DuBuc et al., 2020; Lohmann et al., 1999; Masuda-
102   Ozawa et al., 2022; Quiroga-Artigas et al., 2020) and anthozoans (Dunn et al., 2007; He et al.,
103   2018; Yuyama et al., 2021). Recently, short hairpin RNAs (shRNA) have become a widely
104   adopted approach for RNA interference as they can be synthesized in the lab, thereby enabling
105   cost-effective silencing of numerous target genes (He et al., 2018). We tested the efficacy of
106   shRNA knockdown in *A. poculata* by inhibiting the activity of Fibroblast growth factor A1
107   (FgfA1). In *N. vectensis*, the role of FGF signaling during embryonic patterning has been well-
108   studied (Gilbert et al., 2022; Rentzsch et al., 2008; Sinigaglia et al., 2015) and this pathway is
109   known to be required for the formation of the apical tuft, a sensory structure at the aboral end of
110   the larva from which a group of long cilia emerge (Rentzsch et al., 2008). While the apical tuft is
111   found throughout sea anemones, most coral larvae lack this structure. The presence of an
112   apical tuft in the larval stage of *A. poculata* (Szmant-Froelich et al., 1980) provides an
113   opportunity to investigate the developmental mechanisms driving the convergent evolution of
114   this structure across anthozoans.
115
116   To inhibit Fgf1A function in *A. poculata*, we injected zygotes with either a shRNA targeting the 3'
117   end of the FgfA1 transcript (see Materials and Methods) or a scrambled control shRNA
118   (Karabulut et al., 2019). Animals were then raised to the larval stage at room temperature and
119   inspected for evidence of an apical tuft. At 48 hours post fertilization (hpf), 10/10 of the
120   knockdown larvae lacked apical tuft cilia, consistent with an inhibition of FgfA1 function (**Fig
121   2A**). To further confirm the role of FgfA1 in regulating apical tuft development, we treated a
122   separate group of zygotes with the MEK/ERK inhibitor SU5402 (20μM), which has previously
123   been shown to inhibit FgfA1-mediated control of apical tuft development in *N. vectensis*
124   (Rentzsch et al., 2008). Treatment with SU5402 effectively phenocopied FgfA1 shRNA
125   knockdown (**Fig 2B**), resulting in the complete loss of an apical tuft in 12/12 larvae at 48hpf.
126   These phenotypes were quantified by measuring the length of the longest cilium at the aboral

127 end of each larva. The aboral cilia of the FgfA1 knockdown animals were significantly shorter
128 than those in both the wild type and control shRNA-injected larvae (**Fig 2C**). Likewise, we
129 observed a significant reduction in the length of cilia at the aboral pole in SU5402-treated
130 larvae, relative to DMSO controls (Fig 2C). These experiments demonstrate that shRNA
131 injection is a robust method for gene knockdown in corals and confirm that apical tuft
132 development requires similar signaling pathways in two distantly related anthozoans (*N.*
133 *vectensis* and *A. poculata*) **(Fig 2D)**. Pharmacological inhibition of FGF signaling has also been
134 shown to inhibit settlement and metamorphosis in *Acropora millepora*, a species that lacks an
135 apical tuft (Cleves et al., 2018; Strader et al., 2018). With access to this inexpensive and robust
136 method for gene knockdown it is now possible to interrogate the evolution of the FGF signaling
137 pathway controlling apical sensory organ development in cnidarians with diverse larval body
138 plans.
139
140 **Development of a transgenic knock-in coral to study cnidocyte development**
141 Genome editing approaches using CRISPR/Cas9 technology have already been used for loss-
142 of-function analysis in a variety of cnidarians including the sea anemone *Nematostella*
143 *vectensis*, the hard coral *Acropora millepora,* and the hydroids *Hydractinia symbiolongicarpus*
144 and *Clytia hemisphaerica* (Cleves et al., 2018; Gahan et al., 2017; Ikmi et al., 2014; Momose et
145 al., 2018). Endogenous tagging of native proteins with fluorescent markers using CRISPR-
146 mediated homology-directed repair (HDR) has further enabled precise tagging of individual
147 proteins and careful analysis of protein activity in vivo in *N. vectensis* and *H. symbiolongicarpus*
148 (Ikmi et al., 2014; Paix et al., 2023; Sanders et al., 2018). To date, however, successful gene
149 knock-in in corals has not been reported. To establish a method for CRISPR-mediated gene
150 knock-in in *A. poculata*, we tested a method that uses PCR-generated micro-homology
151 fragments to induce HDR after CRISPR-Cas9 cleavage (Seleit et al., 2021). The benefit of this
152 method is that knock-in repair templates can be constructed rapidly and inexpensively by PCR,
153 without the need for cloning. To test the efficacy of CRISPR-mediated knock-in, we tagged the
154 cnidocyte-specific marker gene, Minicollagen3 (*Mcol3*), with the fluorescent protein,
155 mNeonGreen (mNeon). Minicollagens are found only in cnidocytes, making the expression of
156 *Mcol3* a specific and robust marker of cnidocyte development (David et al., 2008).
157
158 We designed two single guide RNAs (sgRNAs) targeting the stop codon of the last exon of
159 *Mcol3* and used an HDR repair template to insert the sequence of mNeon downstream of and in
160 frame with *Mcol3* (**Fig 3A**). After injecting this repair template along with the sgRNAs and Cas9
161 protein, we observed positive fluorescent signal in developing cnidocytes beginning at 36hpf in
162 approximately 10% (8/80) of injected larvae (**Fig 3B**). Most of the knock-in larvae (7/8) exhibited
163 mosaic expression of Mcol3::mNeon, a common outcome of CRISPR-mediated genome editing
164 likely representing a repair event that occurred at later embryonic stages. We confirmed positive
165 integration using PCR with primers that flank mNeon to discriminate wild type alleles from
166 mutant alleles with gel electrophoresis (**Fig 3C**). Using *in situ* hybridization, we confirmed that
167 the knock-in construct recapitulated endogenous expression, showing that *Mcol3* is expressed
168 in a salt and pepper pattern in the ectoderm during embryogenesis in *A. poculata* (**Fig 3D**), a
169 pattern consistent with the development of cnidocytes in *N. vectensis* (Zenkert et al., 2011).
170 Mature cnidocytes are visible in the larva at 48 hpf, shortly after the onset of expression of
171 *Mcol3* (**Fig 3E**). Together, these data show that the timing and distribution of fluorescent cells
172 observed in knock-in larvae are consistent with the endogenous expression of *Mcol3* mRNA in
173 *A. poculata* and the appearance of mature cnidocytes in wild type larvae. Cnidocytes are
174 thought to have evolved from a neural-like precursor in the ancestor of cnidarians (Babonis et
175 al., 2022), yet our understanding of the complex regulatory interactions that drive diversification
176 of cnidocyte form and function remains limited (Babonis et al., 2023). The ability to track early

177 cnidocyte development in vivo using endogenously tagged proteins in *A. poculata* makes this
178 animal a critical model for understanding diversification of this phylum-restricted cell type.
179
180 **Conclusions**
181 Due to the ease of collection and the ability to control the timing of spawns in the lab, *Astrangia*
182 *poculata* is a tractable organism for functional genomic studies in hard corals. Their hardy,
183 transparent embryos are robust to microinjection and genetic manipulation. We show that gene
184 silencing and overexpression can be achieved by microinjection using low-cost techniques. We
185 also show that exogenous gene knock-in can be readily achieved using a repair template
186 generated by PCR to induce HDR following a CRISPR/Cas9 cutting reaction. The toolset
187 presented here enables future studies of development in *A. poculata*, which has recently been
188 recognized as a valuable experimental system for investigative studies of coral-microbe studies
189 (Puntin et al., 2022), as a tractable research organism for functional studies in corals and, more
190 broadly, as a viable system for comparative studies of cnidarian evolution and development (**Fig**
191 **4**). Additionally, we show that *A. poculata* is a valuable organism for studies of comparative
192 developmental biology in cnidarians as this animal shares some larval features in common with
193 *N. vectensis* and shares other features in common with other corals. We anticipate that the
194 functional genomic techniques described here can be readily adapted for studying early
195 development in other coral species and will accelerate research on fundamental cellular and
196 molecular processes in corals and enable finer scale comparisons of comparative development
197 in Anthozoa.
198
199 **Acknowledgements**
200 This work was supported by the North Carolina Biotechnology Center (2022-FLG-3803, J.F.W.)
201 and the National Institutes of Health (R15GM139113-01A1 to J.F.W., R35GM147253-01 to
202 L.S.B., and P20GM103430 to K.S.)
203
204 **Author Contributions**
205 JFW, RB, AS, EB, IVC, KS and LSB collected data and performed analyses; JFW and LSB
206 conceived of the study and wrote the manuscript; RB, AS, EB, IVC, and KS edited and
207 approved the manuscript.
208
209 **Declaration of Interests**
210 The authors declare no competing interests.
211
212 **Data and Code Availability**
213 The transcriptome assembly used for cloning, primer design, and knock-in construct design has
214 been deposited at the NCBI repository (PRJNA956119) and is publicly available as of the date
215 of publication. All transcript, primer, and donor sequences associated with this manuscript are
216 provided in the Methods.
217
218
219

220 **Figures**
221
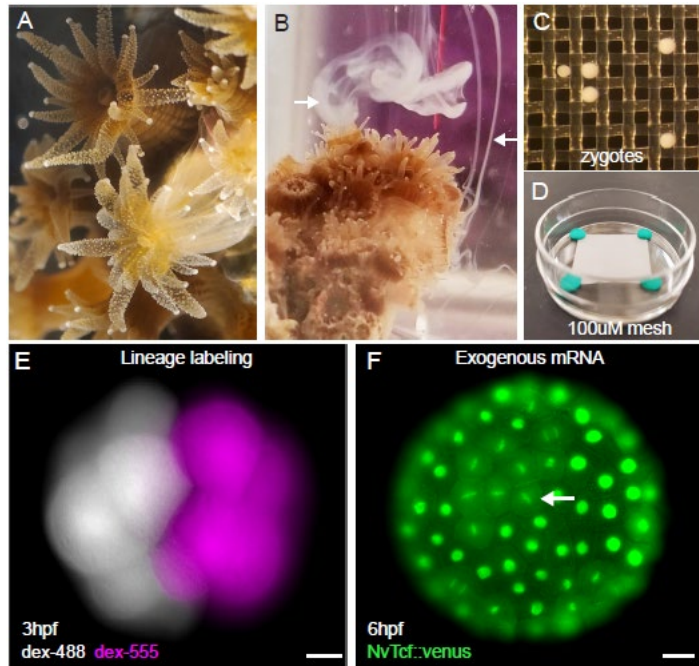
222
223 **Fig. 1.** *Astrangia poculata* is a tractable research organism for functional molecular studies in
224 corals. (A) *A. poculata* colony showing extended polyps. (B) *A. poculata* colony during
225 spawning; arrows point to sperm emerging from two polyps. (C,D) Zygotes resting on nylon
226 mesh fixed in the bottom of a 35mm petri dish in preparation for microinjection. (E) Live image
227 of a 16-cell stage embryo injected at the 2-cell stage with two different dextran dyes (dex-488,
228 dex-555). (F) Injection of mRNA encoding a TCF-venus fusion protein from *Nematostella*
229 *vectensis* (NvTCF::venus) demonstrates proper translation and nuclear localization of
230 exogenous mRNAs; arrow points to cells in M-phase. Scale bars = 20µm.
231
232
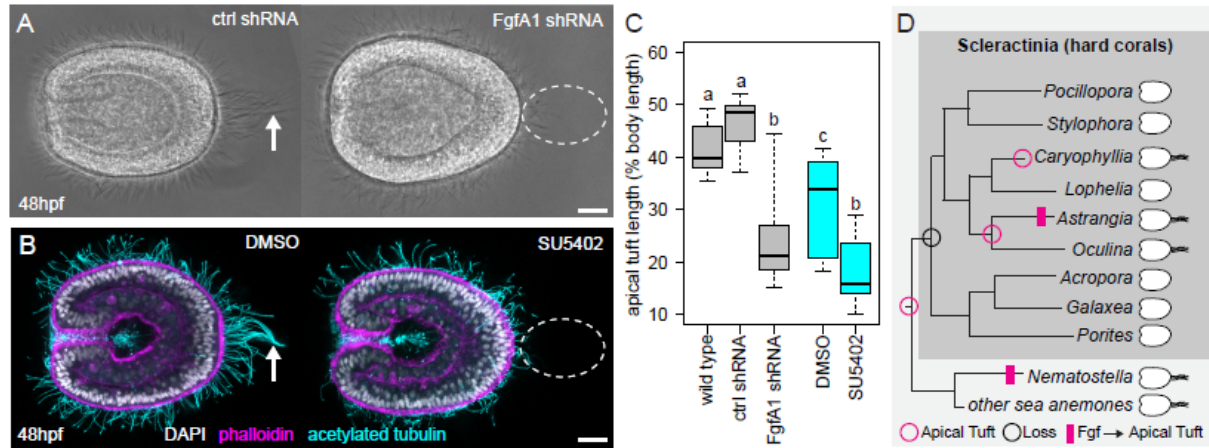
Fig. 2. Knockdown of FgfA1 induces loss of the apical tuft. (A) Live images of 48 hpf larvae injected with scrambled control shRNA (ctrl shRNA) or FgfA1 shRNA. (B) Images of fixed, 48 hpf larvae treated with 20μM SU5402 or vehicle control (DMSO) and stained with DAPI (nuclei), phalloidin (F-actin), and anti-acetylated tubulin antibody (cilia). Arrows in A,B point to apical tuft cilia and dotted circles indicate loss of apical tuft. The oral pole is to the left in A,B; scale bars = 20μm. (C) Quantitative analysis of apical tuft cilia length in the shRNA experiment (grey boxes) and pharmacological experiment (cyan boxes). Box plots are presented as: median – middle line, 25th and 75th percentiles – box, 5th and 95th percentiles – whiskers. Sample sizes for each treatment: wild type N=10, ctrl shRNA N=8, FgfA1 shRNA N=10, DMSO N=10, SU5402 N=12. P-values from ANOVA with TukeyHSD posthoc: wild type vs. ctrl shRNA: p=0.5839021, wild type vs FgfA1 shRNA: p=0.0000064, ctrl shRNA vs FgfA1 shRNA: p= 0.0000001, wild type vs DMSO: p= 0.0154365, DMSO vs SU5402: p= 0.0004114, FgfA1 shRNA vs SU5402: p= 0.3147784. Letters indicate groups that are significantly different. (D) Cladogram of hard corals and sea anemones plotting the distribution of taxa with a larval apical tuft (cartoons, right). The apical tuft was likely lost in the ancestor of Scleractinia (black circle) and regained in the ancestor of the clade containing *Astrangia* and *Oculina* and at least one species of Caryophyllia (magenta circles). An Fgf signaling pathway controls apical tuft development in *Astrangia poculata* (this study) and *Nematostella vectensis* (Rentzsch et al., 2008). The cladogram was inferred from two studies of overlapping taxa (Kitahara et al., 2010; McFadden et al., 2021). References indicating presence/absence of apical tuft by taxon: *Pocillopora* (Tran and Hadfield, 2013), *Stylophora* (Atoda, 1951), *Caryophyllia* (Tranter et al., 1982), *Lophelia* (Larsson et al., 2014), *Astrangia* (Szmant-Froelich et al., 1980), *Oculina* (Brooke and Young, 2003), *Acropora* (Hayward et al., 2015), *Galaxea* (Atoda, 1951), *Porites* (Santiago-Valentín et al., 2022), *Nematostella* (Hand and Uhlinger, 1992), other sea anemones: *Anthopleura* (Chia and Koss, 1979), *Exaiptasia* (Bucher et al., 2016), *Gonactinia* (Chia et al., 1989).
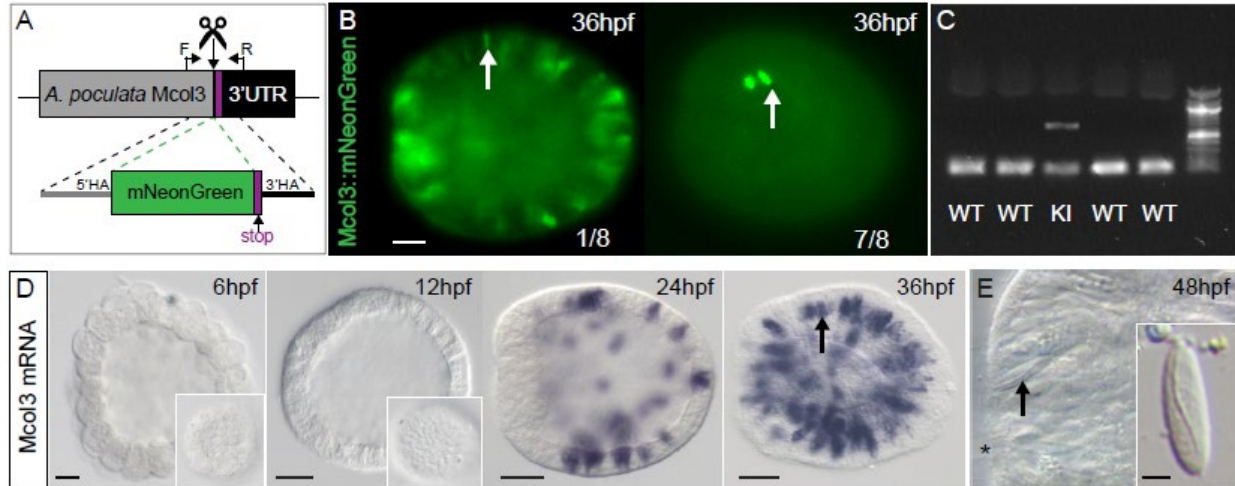
Fig. 3. Endogenous labeling of developing cnidocytes using CRISPR/Cas9 genome editing. (A) Schematic showing knock-in strategy with relative position of sgRNA (scissors), genotyping primers (F/R, bent arrows), and repair template, including left and right homology arms (5'HA, 3'HA). The stop codon is indicated in purple. (B) Live images of embryos exhibiting either complete (1/8 embryos) or mosaic (7/8 embryos) fluorescent expression of *Mcol3*::mNeon; labeled cnidocytes (arrows) are distributed throughout the ectoderm. (C) Agarose gel genotyping of five individual embryos, one knock-in mutant (KI) and four wild types (WT). The wild type amplicon (350 bp) is present in all five embryos and the amplicon containing the mNeon insert (1060 bp) is present only in the mutant. (D) *In situ* hybridization confirms the timing and distribution of cells expressing *Mcol3* mRNA (immature cnidocytes) in the ectoderm at/after 24 hpf. Insets show surface detail and arrow points to *Mcol3*-expressing immature cnidocytes. (E) Mature cnidocytes are detected in the ectoderm at 48 hpf. DIC image of the oral region of a 48 hpf larva. Inset shows an isolated cnidocyte extracted from a dissociated larva; arrow points to a mature cnidocyte in situ. The oral pole is to the left in B,D-E; the position of the blastopore is marked by * in E. Scale bars in B,D = 20μm; scale bar in E = 2μm.
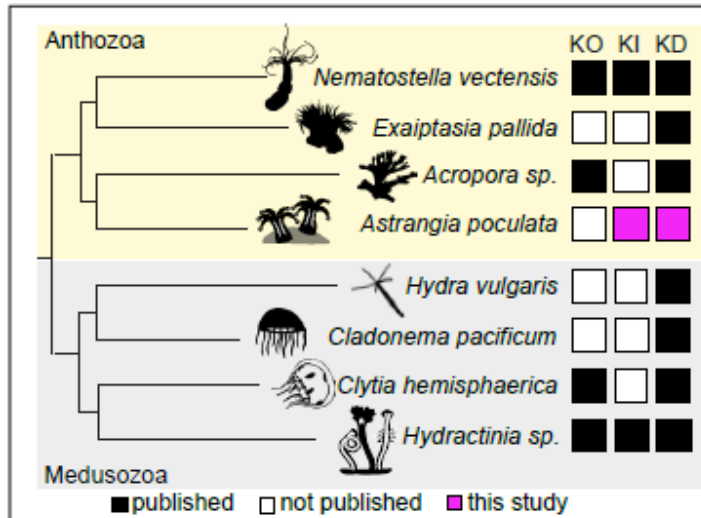
Fig. 4. Summary of functional genomic tools available in cnidarians. KO – knockout, KI – knock-in, KD – knockdown by RNA interference. References by taxon: *Nematostella vectensis* (He et al., 2018; Ikmi et al., 2014), *Exaiptasia pallida* (Dunn et al., 2007), *Acropora millepora* (KO) (Cleves et al., 2018), *Acropora tenuis* (KD) (Yuyama et al., 2021), *Astrangia poculata* (this study), *Hydra vulgaris* (Lohmann et al., 1999), *Cladonema pacificum* (Masuda-Ozawa et al., 2022), *Clytia hemisphaerica* (KO) (Momose et al., 2018; Quiroga Artigas et al., 2018), *Clytia hemisphaerica* (KD) (Masuda-Ozawa et al., 2022), *Hydractinia echinata* (KO) (Gahan et al., 2017), *Hydractinia symbiolongicarpus* (KI,KD) (DuBuc et al., 2020; Quiroga-Artigas et al., 2020; Sanders et al., 2018). The cladogram was inferred from two studies of overlapping taxa (Fang et al., 2022; Kayal et al., 2018). Silhouettes were downloaded from Phylopic.org, license (CC BY-SA 3.0).

Materials and Methods

Animal collection and maintenance. Fresh colonies of *A. poculata* were collected by divers from Ft. Wetherill, RI, USA and transferred to Roger Williams University. Spawning was induced by acute heat shock (27-28°C for 1 hour) in benchtop containers. After spawning, adult colonies were maintained in a flow-through system with natural seawater and a 12:12 light cycle at Roger Williams University, Bristol, RI.

Microinjection. *Astrangia poculata* gametes were collected and fertilized in 0.2um-filtered sea water and then transferred in filtered seawater to a 35mm petri dish containing 100μm mesh (Sefar Nitex 03-100/32) secured to the bottom using modeling clay. Individual zygotes were injected using a fluorescent Zeiss Discovery V8 dissecting scope, Narishige micromanipulator, and Eppendorf FemtoJet 4i picospritzing device, following a protocol developed previously for *N. vectensis* (Layden et al., 2013). Two different dextran dyes (Alexa 555 and Alexa 488 - Invitrogen D34679, D22910) each diluted to a final concentration of 0.2mg/ml in nuclease free water (Ambion AM9937) were used to mark individual blastomeres by injection at the two-cell stage. To assess the feasibility of expressing heterologous mRNA in *A. poculata*, zygotes (one-cell stage) were injected with mRNA encoding a NvTCF-venus fusion protein construct (Röttinger et al., 2012) diluted to 300ng/ul with 0.2mg/ml RNAse-free dextran in nuclease free water. Injected embryos were reared at room temperature (~ 22°C) for both experiments, mounted in filtered sea water on glass slides, and imaged live on a Nikon Eclipse E800 fluorescent microscope at Roger Williams University.

Transcriptome assembly. Larvae were collected at 12 hpf, 24 hpf, 36 hpf, 60 hpf, and 84 hpf in Tri-reagent (Sigma T9424) and stored at -80°C prior to RNA extraction. Total RNA was purified following a protocol previously described for *N. vectensis* (Layden et al., 2013). Briefly, samples were processed through two phenol/chloroform extractions and precipitated in isopropanol before being treated for DNA contamination with Turbo-DNAse (Ambion AM1907) for 10 in at 37°C. Library preparation and 150 bp PE illumina sequencing (NovaSeq 6000) was carried out by Novogene. Sequencing reads were combined and error corrected using Rcorrector (Song and Florea, 2015). Adapter trimming and quality trimming were carried out using Cutadapt v3.7 (Martin, 2011) and Trimmomatic v.039 (Bolger et al., 2014), respectively. Cleaned reads were filtered for ribosomal sequences by aligning them ribosomal sequences for *A. poculata* from the SILVA database (Quast et al., 2013) using Bowtie2 v2.3.4.1 (Langmead and Salzberg, 2012). Unaligned reads were input into Trinity v2.12.0 (Grabherr et al., 2011) for assembly and final, assembled transcripts were filtered for sequences longer than 200 bp. Raw sequencing reads and assembled transcripts have been deposited to NCBI under bioproject: PRJNA956119.

shRNA design and synthesis. The *A. poculata* ortholog of FgfA1 was identified using TBLASTN with the *N. vectensis* FGFA1 peptide sequence (NCBI accession: ABN70831.1) as query and the *A. poculata* assembled transcripts as reference. shRNAs were designed and synthesized as described previously for *N. vectensis* (He et al., 2018). In brief, primers were designed to target the 3' end of the FgfA1 coding sequence using the Invivogen siRNA Wizard (www.invivogen.com/sirnawizard/design.php) and annealed for 2 min at 98°C in a thermocycler to generate a template for in vitro transcription. Transcription was performed using the Lucigen Campliscribe T7 Flash kit (ASF3257) for 5h at 37°C in a thermocycler, following the manufacturer's instructions. Products were column-purified using the Zymo Direct-zol RNA Miniprep Kit (R2050), aliquoted, and frozen at -80 C until the day of microinjection. A scrambled control shRNA was synthesized at the same time using primers described previously (Karabulut

346 et al., 2019). All shRNAs were injected into zygotes at a concentration of 800ng/ul with
347 0.2mg/ml RNAse-free dextran in nuclease-free water. Embryos were reared to 48 hpf at room
348 temperature, mounted in filtered seawater on glass slides, and imaged live on a Nikon Eclipse
349 E800 at Roger Williams University. Primer sequences for FgfA1 shRNA synthesis are:

350
351 Apoc_FgfA1_shRNA_F:
352 TAATACGACTCACTATAGACAACAGCCGCATGACATTTCAAGAGAATGTCATGCGGCTGTTGTCTT
353 Apoc_FgfA1_shRNA_R:
354 AAGACAACAGCCGCATGACATTCTCTTGAAATGTCATGCGGCTGTTGTCTATAGTGAGTCGTATTA

355
356 **Fgf inhibitor treatment.** Beginning immediately after fertilization, zygotes were incubated in
357 0.1% DMSO in filtered seawater containing 20mM SU5402 (Sigma SML0443) for a final
358 concentration of 20μM SU5402 or 0.1% DMSO in filtered sea water (control). Embryos were
359 reared at room temperature and solutions were refreshed every 24 hours until embryos were
360 collected and fixed for immunostaining (48 hpf).

361
362 **Immunostaining.** *Astrangia poculata* larvae were fixed in 4% paraformaldehyde (PFA) in
363 filtered seawater and washed four times in phosphate buffered saline with 0.1% Tween-20
364 (PTw) for five minutes each. Non-specific protein interactions were blocked in 10% normal goat
365 serum (NGS) diluted in PTw for 1 hour at room temperature. The blocking solution was replaced
366 with a solution containing 1:200 anti-acetylated tubulin antibody (Sigma T6743) diluted in 10%
367 NGS and the samples were incubated overnight at 4°C. Larvae were washed four times using
368 PTw and incubated in a secondary antibody (Invitrogen A11004) diluted 1:200 in 10% NGS for 2
369 hours at room temperature. Larvae were again washed four times using PTw and
370 counterstained in DAPI (Sigma D9542) diluted 1:2,500 and Phalloidin (Invitrogen A12379)
371 diluted 1:200 in PBS overnight at 4°C. Larvae were washed four times in PTw, mounted in 75%
372 glycerol in PBS on glass slides, and imaged on a Leica Sp8 confocal microscope at UNC
373 Wilmington.

374
375 **In situ hybridization.** Embryos from various developmental stages were collected and fixed for
376 in situ hybridization (ISH) using a two-part fixative series. First, embryos were fixed for 1 min at
377 room temperature in 4% PFA in PTw containing 0.25% gluteraldehyde. This initial fixative was
378 removed and replaced with 4% PFA in PTw and embryos were fixed for an additional 1h at 4°C.
379 Excess fixative was removed with three 10-min washes in PTw and tissues were then rinsed
380 once in sterile water to remove excess PTw and twice in 100% methanol before being stored in
381 clean 100% methanol at -20°C until analysis. ISH was performing following a method developed
382 previously for *N. vectensis* (Wolenski et al., 2013), with minor modification. Due the small size
383 and transparency of *A. poculata* embryos, all pipetting steps in the ISH procedure were
384 performed in a sterile 24-well microplate on a dissecting microscope. An antisense mRNA probe
385 directed against the *A. poculata* Mcol3 transcript was synthesized as described for *N. vectensis*
386 (Wolenski et al., 2013) using the following primers:

387
388 Apoc_Mcol3_F:
389 ATGGCGTCTAAACTCATTCTTG
390 Apoc_Mcol3_R:
391 TCACGCGTGCACACACCTA

392
393 Tissues were hybridized overnight with the Mcol3 probe diluted to 1ng/ul in hybridization buffer
394 (Wolenski et al., 2013) and signal was visualized using an NBT/BCIP reaction performed in the
395 dark at room temperature. Labeled embryos were washed extensively in PTw to remove excess

396 NBT/BCIP, mounted in 80% glycerol (in PBS) on glass slides, and imaged on a Nikon Eclipse
397 E800 at Cornell University.

398

399 **CRISPR-mediated knock-in.** The *A. poculata* ortholog of *Mcol3* was identified using TBLASTN
400 with the *N. vectensis* MCOL3 peptide sequence (NCBI accession: XP_032218917.1; Uniprot
401 accession: G7H7X1) as query and the *A. poculata* assembled transcripts as reference. The
402 open reading frame was predicted using the NCBI Open Reading Frame Finder
403 (https://www.ncbi.nlm.nih.gov/orffinder/) and sgRNAs targeting the C-terminus of the predicted
404 peptide were designed using ChopChop v3 (Labun et al., 2019). Two overlapping guides were
405 designed with the recognition sites CGTGGTCGCTTACTTTCTGC and AATGTCGACGCATCATCACG
406 that cut 4bp upstream and 11bp downstream from the insertion site respectively. Single guide
407 RNAs (sgRNAs) were synthesized by Synthego (Redwood City, CA, USA) with the default 2'-O-
408 Methyl modification at the 3 first bases and 3' phosphorothioate bonds between the first three
409 and last two bases.

410

411 Knock-in repair templates were synthesized using PCR. To do this, primers were designed to
412 contain 40 bp homology arms that are homologous to the insertion site (immediately 5' and 3' to
413 the predicted stop codon), a two-alanine spacer, and 15 bp to bind and amplify mNeonGreen in
414 frame with the open reading frame. Silent mutations were introduced in the sgRNA recognition
415 sequences to prevent recutting from sgRNAs. The oligo sequences were as follows (*Apoc*
416 homology sequences, sgRNA mutations, [linker], **mNeon priming region**):

417

418 Apoc_Mcol3_Homology_F:
419 5'GCGTCTCGTCCTGCCCGACCCAGTGCTGCTCCGGGAGGAAA[GCCGCA]**ATGGTGAGCAAGGGC**3'
420 Apoc_Mcol3_Homology_R:
421 5'TAATTTCTAAATCTCGTGCTAATGTCGACGCATCAAGTGCTCGTGGC**TTACTTGTACAGCTCGTC**3'

422

423 PCR amplification of the repair template was performed using 50 ng of plasmid containing
424 mNeonGreen (Addgene 125134) as template in a touchdown PCR reaction (annealing
425 temperature decreased 1°C from 65°C to 50°C for the first 15 cycles followed by 20 cycles with
426 an annealing temperature of 50°C; extension time was 30s). Afterwards, the template was
427 digested by addition of DpnI enzyme (NEB R0176S) and incubation at 37°C for 2 hours. The
428 repair template was then purified using a QiaQuick PCR purification kit (Qiagen 28704) prior to
429 injection and quality assessed using agarose gel electrophoresis, to ensure size, and Nanodrop,
430 to assess purity and concentration.

431

432 The injection mix was assembled as follows:
433 150ng/ul final concentration of dsDNA repair template
434 200ng/ul final concentration of ApMcol3 sgRNA1
435 200ng/ul final concentration of ApMcol3 sgRNA2
436 0.5ul of Cas9 protein (IDT 1081060)
437 Alexa-555 dextran (0.2mg/ml)
438 Nuclease free water to 5ul

439

440 Ribonucleoprotein (RNP) assembly was promoted by incubation of the injection mix at room
441 temperature for 15 minutes prior to injection.

442

443 **Imaging and genotyping knock-in mutants.** Mutant embryos were identified using a
444 fluorescent dissecting scope, mounted on glass slides in filtered sea water, and imaged live on
445 a Nikon Eclipse E800 fluorescent microscope at Roger Williams University. Selected mutant

446 knock-in larvae (48 hpf) were transferred individually to 0.5ml PCR tubes and gDNA was
447 extracted from individual larvae as previously described (Servetnick et al., 2017). PCR was
448 used to amplify the knock-in locus and insert size was confirmed using gel electrophoresis.
449 Genotyping primers are as follows:
450
451 `Apoc_Mcol3NG_F:`
452 `GGACCATCTGGACGAATGGGAC`
453 `Apoc_Mcol3NG_R:`
454 `CAATTCGCTCTTCTCTGCCTTCTAT`
455
456 **Predicted gene sequences:**
457 *Astrangia poculata* Minicollagen 3 (constructed from multiple overlapping assembled transcripts,
458 *= stop codon location):
459 `ATGAAAGACTCAACGACTGTCGAAATACAGCCTTATTCAAGCACATTTCAAAGATCGCTAGCCTGGGATC`
460 `CAGAGATGGCGTCTAAACTCATTCTTGGGTGCTTAGCACTCATGGTAGTGTCGACCTACGCCAGATCAAC`
461 `ATACAAAAGAAGCGCTAACCCGTGTCCCCCGGGATGTCCCGGTAGTTGTGCGCCCTCGTGTGCGGTGTCT`
462 `TGTTGTCTTCCTCCACCACCCGCTCCACCACCGCCCCCACCCCCACCCCCACCACCACCAGAGCCCGCTA`
463 `AGCCCGGACCACCTGGACCATCTGGACGAATGGGACCACCCGGACCTGTCGGACCTATCGGACCCATGGG`
464 `AGAGGCCGGACCACCTGGAATACCCGGACCCCAAGGACCTCCTGGACCTCCCGGAGAACCCGCTCCTCCA`
465 `CCACCACCACCCCCACCGTGCCCACCTGTCTGCGCCCACACATGCGTCTCGTCCTGCCCGACCCAGTGCT`
466 `GCTCCGGCAGAAAGTAA*GCGACCACGTGATGATGCGTCGACATTAGCACGAGATTTAGAAATTACTCCA`
467 `ACTTTAGCGTTCGTAAAGTACTTTTTCAGTGGA`
468
469 *Astrangia poculata* FGF1A (CDS extracted from transcript TRINITY_DN12668_c0_g1_i4):
470 `ATGAATTCCATTCAACTGCTTTTCCTACTTCAACTCTTTTGCTTCACGGAGATAAACACTTCAGCTAAAC`
471 `CGTACAACGCAACCAAATCCCAGACTAAAGATGCCGCGAGAACTTCAAGAGGATCTATCTCATCATCCAT`
472 `GACCAGATACGAAAACGACAGAATCAGAAACCATTCCCGAAAAACATTTCTTTCCAAGAAGCAGAAATGG`
473 `CCACAACCGTCCACGGAAAGTTCCTTGAAACGTGTCCGCAAAATAACAAAACGACCGACAGCTACAACGC`
474 `ACTGTAAAATATTCTGCCGCAGCGGTTATCATCTTCAAATCCTTCCCAGTGGTGCAGTGAGGGGGACGGT`
475 `TGACCAGGGCAGCAAGTACGTGTTGTTTGAGATGCAGTCATTTGGCCCTAGTCTCGTCAGGCTGATGAGT`
476 `ACAGCGACGGGCAGGTACCTATCTATGAGAAGAGACGGGAGTCTTCGAGGGTTGCGTAGCCAAAGTAACC`
477 `GGGACTCACTTTTCAAAGAGACACATGAACAGAACGCGTTTCACTCTTACGCGTCACACAGATATTACAG`
478 `ACAACAGCCGCATGACATGTTGGTTGGCATCAAGAGAAACGGACAAATAAAACGAGCCACTAAAACCTTG`
479 `CATGGACAAACTGCTACGCAATTTCTTGTCATCAAATTTTAA`
480
481 **Quantification and Statistical Analysis.** Quantitative analysis of apical tuft morphology was
482 performed by measuring the maximum length of the longest aboral cilium and the length of the
483 body axis (mouth to apical tuft base) in individual embryos using the Measure Tool in Fiji V1.54b
484 (Schindelin et al., 2012). All data were analyzed in the R statistical computing environment
485 V4.2.1 (R Core Team, 2020).
486

487 **References**
488 **Atoda, K.** (1951). The larva and postlarval development of the reef-building corals IV. Galaxea
489 aspera quelch. *J. Morphol.* **89**, 17–35.
490 **Babonis, L. S., Enjolras, C., Ryan, J. F. and Martindale, M. Q.** (2022). A novel regulatory
491 gene promotes novel cell fate by suppressing ancestral fate in the sea anemone
492 Nematostella vectensis. *Proc. Natl. Acad. Sci.* **119**, e2113701119.

Babonis, L. S., Enjolras, C., Reft, A. J., Foster, B. M., Hugosson, F., Ryan, J. F., Daly, M. and Martindale, M. Q. (2023). Single-cell atavism reveals an ancient mechanism of cell type diversification in a sea anemone. *Nat. Commun.* **14**, 885.

Bolger, A. M., Lohse, M. and Usadel, B. (2014). Trimmomatic: a flexible trimmer for Illumina sequence data. *Bioinformatics* **30**, 2114–2120.

Brooke, S. and Young, C. (2003). Reproductive ecology of a deep-water scleractinian coral, Oculina varicosa, from the southeast Florida shelf. *Cont. Shelf Res.* **23**, 847–858.

Bucher, M., Wolfowicz, I., Voss, P. A., Hambleton, E. A. and Guse, A. (2016). Development and Symbiosis Establishment in the Cnidarian Endosymbiosis Model Aiptasia sp. *Sci. Rep.* **6**, 19867.

Chia, F.-S. and Koss, R. (1979). Fine structural studies of the nervous system and the apical organ in the planula larva of the sea anemone Anthopleura elegantissima. *J. Morphol.* **160**, 275–297.

Chia, F.-S., Lützen, J. and Svane, I. (1989). Sexual reproduction and larval morphology of the primitive anthozoan Gonactinia prolifera M. Sars. *J. Exp. Mar. Biol. Ecol.* **127**, 13–24.

Cleves, P. A., Strader, M. E., Bay, L. K., Pringle, J. R. and Matz, M. V. (2018). CRISPR/Cas9-mediated genome editing in a reef-building coral. *Proc. Natl. Acad. Sci.* **115**, 5235–5240.

Crawford, K., Diaz Quiroz, J. F., Koenig, K. M., Ahuja, N., Albertin, C. B. and Rosenthal, J. J. C. (2020). Highly Efficient Knockout of a Squid Pigmentation Gene. *Curr. Biol. CB* **30**, 3484-3490.e4.

David, C. N., Özbek, S., Adamczyk, P., Meier, S., Pauly, B., Chapman, J., Hwang, J. S., Gojobori, T. and Holstein, T. W. (2008). Evolution of complex structures: minicollagens shape the cnidarian nematocyst. *Trends Genet.* **24**, 431–438.

Dimond, J., Kerwin, A., Rotjan, R., Sharp, K., Stewart, F. and Thornhill, D. (2013). A simple temperature-based model predicts the upper latitudinal limit of the temperate coral Astrangia poculata. *Coral Reefs* **32**, 401–409.

DuBuc, T. Q., Schnitzler, C. E., Chrysostomou, E., McMahon, E. T., Febrimarsa, Gahan, J. M., Buggie, T., Gornik, S. G., Hanley, S., Barreira, S. N., et al. (2020). Transcription factor AP2 controls cnidarian germ cell induction. *Science* **367**, 757–762.

Dunn, S. R., Phillips, W. S., Green, D. R. and Weis, V. M. (2007). Knockdown of Actin and Caspase Gene Expression by RNA Interference in the Symbiotic Anemone Aiptasia pallida. *Biol. Bull.* **212**, 250–258.

Fang, X., Zhou, K. and Chen, J. (2022). The complete linear mitochondrial genome of the hydrozoan jellyfish Cladonema multiramosum Zhou et al., 2022(Cnidaria: Hydrozoa: Cladonematidae). *Mitochondrial DNA Part B Resour.* **7**, 921–923.

Fritzenwanker, J. H., Genikhovich, G., Kraus, Y. and Technau, U. (2007). Early development and axis specification in the sea anemone Nematostella vectensis. *Dev. Biol.* **310**, 264–279.

Gahan, J. M., Schnitzler, C. E., DuBuc, T. Q., Doonan, L. B., Kanska, J., Gornik, S. G., Barreira, S., Thompson, K., Schiffer, P., Baxevanis, A. D., et al. (2017). Functional studies on the role of Notch signaling in Hydractinia development. *Dev. Biol.* **428**, 224–231.

Gilbert, E., Teeling, C., Lebedeva, T., Pedersen, S., Chrismas, N., Genikhovich, G. and Modepalli, V. (2022). Molecular and cellular architecture of the larval sensory organ in the cnidarian Nematostella vectensis. *Dev. Camb. Engl.* **149**, dev200833.

Grabherr, M. G., Haas, B. J., Yassour, M., Levin, J. Z., Thompson, D. A., Amit, I., Adiconis, X., Fan, L., Raychowdhury, R., Zeng, Q., et al. (2011). Full-length transcriptome assembly from RNA-Seq data without a reference genome. *Nat. Biotechnol.* **29**, 644–652.

Hand, C. and Uhlinger, K. R. (1992). The Culture, Sexual and Asexual Reproduction, and Growth of the Sea Anemone *Nematostella vectensis*. *Biol. Bull.* **182**, 169–176.

Hayward, D. C., Grasso, L. C., Saint, R., Miller, D. J. and Ball, E. E. (2015). The organizer in evolution–gastrulation and organizer gene expression highlight the importance of Brachyury during development of the coral, Acropora millepora. *Dev. Biol.* **399**, 337–347.

He, S., del Viso, F., Chen, C.-Y., Ikmi, A., Kroesen, A. E. and Gibson, M. C. (2018). An axial Hox code controls tissue segmentation and body patterning in *Nematostella vectensis*. *Science* **361**, 1377–1380.

Ikmi, A., McKinney, S. A., Delventhal, K. M. and Gibson, M. C. (2014). TALEN and CRISPR/Cas9-mediated genome editing in the early-branching metazoan Nematostella vectensis. *Nat. Commun.* **5**, 5486.

Karabulut, A., He, S., Chen, C.-Y., McKinney, S. A. and Gibson, M. C. (2019). Electroporation of short hairpin RNAs for rapid and efficient gene knockdown in the starlet sea anemone, Nematostella vectensis. *Dev. Biol.* **448**, 7–15.

Kayal, E., Bentlage, B., Sabrina Pankey, M., Ohdera, A. H., Medina, M., Plachetzki, D. C., Collins, A. G. and Ryan, J. F. (2018). Phylogenomics provides a robust topology of the major cnidarian lineages and insights on the origins of key organismal traits. *BMC Evol. Biol.* **18**, 68.

Kitahara, M. V., Cairns, S. D., Stolarski, J., Blair, D. and Miller, D. J. (2010). A Comprehensive Phylogenetic Analysis of the Scleractinia (Cnidaria, Anthozoa) Based on Mitochondrial CO1 Sequence Data. *PLOS ONE* **5**, e11490.

Labun, K., Montague, T. G., Krause, M., Torres Cleuren, Y. N., Tjeldnes, H. and Valen, E. (2019). CHOPCHOP v3: expanding the CRISPR web toolbox beyond genome editing. *Nucleic Acids Res.* **47**, W171–W174.

567 **Langmead, B. and Salzberg, S. L.** (2012). Fast gapped-read alignment with Bowtie 2. *Nat.*
568   *Methods* **9**, 357–359.

569 **Larsson, A. I., Järnegren, J., Strömberg, S. M., Dahl, M. P., Lundälv, T. and Brooke, S.**
570   (2014). Embryogenesis and Larval Biology of the Cold-Water Coral Lophelia pertusa.
571   *PLoS ONE* **9**, e102222.

572 **Layden, M. J., Röttinger, E., Wolenski, F. S., Gilmore, T. D. and Martindale, M. Q.** (2013).
573   Microinjection of mRNA or morpholinos for reverse genetic analysis in the starlet sea
574   anemone, Nematostella vectensis. *Nat. Protoc.* **8**, 924–934.

575 **Layden, M. J., Rentzsch, F. and Röttinger, E.** (2016). The rise of the starlet sea anemone
576   *Nematostella vectensis* as a model system to investigate development and regeneration:
577   Overview of starlet sea anemone *Nematostella vectensis*. *Wiley Interdiscip. Rev. Dev.*
578   *Biol.* **5**, 408–428.

579 **Lohmann, J. U., Endl, I. and Bosch, T. C.** (1999). Silencing of developmental genes in Hydra.
580   *Dev. Biol.* **214**, 211–214.

581 **Martin, M.** (2011). Cutadapt removes adapter sequences from high-throughput sequencing
582   reads. *EMBnet.journal* **17**, 10.

583 **Masuda-Ozawa, T., Fujita, S., Nakamura, R., Watanabe, H., Kuranaga, E. and Nakajima, Y.**
584   (2022). siRNA-mediated gene knockdown via electroporation in hydrozoan jellyfish
585   embryos. *Sci. Rep.* **12**, 16049.

586 **McFadden, C. S., Quattrini, A. M., Brugler, M. R., Cowman, P. F., Dueñas, L. F., Kitahara,**
587   **M. V., Paz-García, D. A., Reimer, J. D. and Rodríguez, E.** (2021). Phylogenomics,
588   origin, and diversification of anthozoans (Phylum Cnidaria). *Syst. Biol.* **70**, 635–647.

589 **Momose, T., De Cian, A., Shiba, K., Inaba, K., Giovannangeli, C. and Concordet, J.-P.**
590   (2018). High doses of CRISPR/Cas9 ribonucleoprotein efficiently induce gene knockout
591   with low mosaicism in the hydrozoan Clytia hemisphaerica through microhomology-
592   mediated deletion. *Sci. Rep.* **8**, 11734.

593 **Oulhen, N., Pieplow, C., Perillo, M., Gregory, P. and Wessel, G. M.** (2022). Optimizing
594   CRISPR/Cas9-based gene manipulation in echinoderms. *Dev. Biol.* **490**, 117–124.

595 **Paix, A., Basu, S., Steenbergen, P., Singh, R., Prevedel, R. and Ikmi, A.** (2023).
596   Endogenous tagging of multiple cellular components in the sea anemone Nematostella
597   vectensis. *Proc. Natl. Acad. Sci.* **120**, e2215958120.

598 **Presnell, J. S. and Browne, W. E.** (2021). Krüppel-like factor gene function in the ctenophore
599   Mnemiopsis leidyi assessed by CRISPR/Cas9-mediated genome editing. *Dev. Camb.*
600   *Engl.* **148**, dev199771.

601 **Puntin, G., Sweet, M., Fraune, S., Medina, M., Sharp, K., Weis, V. M. and Ziegler, M.** (2022).
602   Harnessing the power of model organisms to unravel microbial functions in the coral
603   holobiont. *Microbiol. Mol. Biol. Rev. MMBR* **86**, e0005322.

604 **Quast, C., Pruesse, E., Yilmaz, P., Gerken, J., Schweer, T., Yarza, P., Peplies, J. and**
605   **Glöckner, F. O.** (2013). The SILVA ribosomal RNA gene database project: improved
606   data processing and web-based tools. *Nucleic Acids Res.* **41**, D590–D596.

607 **Quiroga Artigas, G., Lapébie, P., Leclère, L., Takeda, N., Deguchi, R., Jékely, G., Momose,**
608   **T. and Houliston, E.** (2018). A gonad-expressed opsin mediates light-induced spawning
609   in the jellyfish Clytia. *eLife* **7**, e29555.

610 **Quiroga-Artigas, G., Duscher, A., Lundquist, K., Waletich, J. and Schnitzler, C. E.** (2020).
611   Gene knockdown via electroporation of short hairpin RNAs in embryos of the marine
612   hydroid Hydractinia symbiolongicarpus. *Sci. Rep.* **10**, 12806.

613 **R Core Team** (2020). R: A language and environment for statistical computing. *R Found. Stat.*
614   *Comput. Vienna Austria*.

615 **Rentzsch, F., Fritzenwanker, J. H., Scholz, C. B. and Technau, U.** (2008). FGF signalling
616   controls formation of the apical sensory organ in the cnidarian *Nematostella vectensis*.
617   *Development* **135**, 1761–1769.

618 **Röttinger, E., Dahlin, P. and Martindale, M. Q.** (2012). A framework for the establishment of a
619   cnidarian gene regulatory network for "endomesoderm" specification: The inputs of ß-
620   Catenin/TCF signaling. *PLoS Genet.* **8**, e1003164.

621 **Sanders, S. M., Ma, Z., Hughes, J. M., Riscoe, B. M., Gibson, G. A., Watson, A. M., Flici, H.,**
622   **Frank, U., Schnitzler, C. E., Baxevanis, A. D., et al.** (2018). CRISPR/Cas9-mediated
623   gene knockin in the hydroid Hydractinia symbiolongicarpus. *BMC Genomics* **19**, 649.

624 **Santiago-Valentín, J.-D, Rodríguez-Troncoso, A.-P., Bautista-Guerrero, E., López-Pérez,**
625   **A., Cupul-Magaña, A.-L., Santiago-Valentín, J.-D., Rodríguez-Troncoso, A.-P.,**
626   **Bautista-Guerrero, E., López-Pérez, A. and Cupul-Magaña, A.-L.** (2022). Internal
627   ultrastructure of the planktonic larva of the coral Porites panamensis (Anthozoa:
628   Scleractinia). *Rev. Biol. Trop.* **70**, 222–234.

629 **Schindelin, J., Arganda-Carreras, I., Frise, E., Kaynig, V., Longair, M., Pietzsch, T.,**
630   **Preibisch, S., Rueden, C., Saalfeld, S., Schmid, B., et al.** (2012). Fiji: an open-source
631   platform for biological-image analysis. *Nat. Methods* **9**, 676–682.

632 **Seleit, A., Aulehla, A. and Paix, A.** (2021). Endogenous protein tagging in medaka using a
633   simplified CRISPR/Cas9 knock-in approach. *eLife* **10**, e75050.

634 **Servetnick, M. D., Steinworth, B., Babonis, L. S., Simmons, D., Salinas-Saavedra, M. and**
635   **Martindale, M. Q.** (2017). Cas9-mediated excision of Nematostella brachyury disrupts
636   endoderm development, pharynx formation, and oral-aboral patterning. *Development*
637   **144**, 2951–2960.

638 **Sinigaglia, C., Busengdal, H., Lerner, A., Oliveri, P. and Rentzsch, F.** (2015). Molecular
639   characterization of the apical organ of the anthozoan Nematostella vectensis. *Dev. Biol.*
640   **398**, 120–133.

641 **Song, L. and Florea, L.** (2015). Rcorrector: efficient and accurate error correction for Illumina
642   RNA-seq reads. *GigaScience* **4**, 48.

643 **Strader, M. E., Aglyamova, G. V. and Matz, M. V.** (2018). Molecular characterization of larval
644   development from fertilization to metamorphosis in a reef-building coral. *BMC Genomics*
645   **19**, 17.

646 **Szmant-Froelich, A., Yevich, P. and Pilson, M. E. Q.** (1980). Gametogenesis and early
647   development of the temperate coral Astrangia danae (Anthozoa: Scleractinia). *Biol. Bull.*
648   **158**, 257–269.

649 **Tinoco, A. I., Mitchison-Field, L. M. Y., Bradford, J., Renicke, C., Perrin, D., Bay, L. K.,**
650   **Pringle, J. R. and Cleves, P. A.** (2023). Role of the bicarbonate transporter SLC4γ in
651   stony-coral skeleton formation and evolution. *Proc. Natl. Acad. Sci.* **120**, e2216144120.

652 **Tran, C. and Hadfield, M. G.** (2013). Localization of sensory mechanisms utilized by coral
653   planulae to detect settlement cues. *Invertebr. Biol.* **132**, 195–206.

654 **Tranter, P. R. G., Nicholson, D. N. and Kinchington, D.** (1982). A Description of Spawning
655   and Post-Gastrula Development of the Cool Temperate Coral, Caryophyllia Smithi. *J.*
656   *Mar. Biol. Assoc. U. K.* **62**, 845–854.

657 **Wolenski, F. S., Layden, M. J., Martindale, M. Q., Gilmore, T. D. and Finnerty, J. R.** (2013).
658   Characterizing the spatiotemporal expression of RNAs and proteins in the starlet sea
659   anemone, Nematostella vectensis. *Nat. Protoc.* **8**, 900–915.

660 **Yuyama, I., Higuchi, T. and Hidaka, M.** (2021). Application of RNA Interference Technology to
661   Acroporid Juvenile Corals. *Front. Mar. Sci.* **8**,.

662 **Zenkert, C., Takahashi, T., Diesner, M.-O. and Özbek, S.** (2011). Morphological and
663   molecular analysis of the Nematostella vectensis cnidom. *PLoS ONE* **6**, e22725.

664